EXTREMAL ANALYTICAL CONTROL AND GUIDANCE SOLUTIONS FOR POWERED DESCENT AND PRECISION LANDING

Dilmurat Azimov

University of Hawaii at Manoa
2540 Dole Street, Holmes 202A
Phone: (808)-956-2863, E-mail: azimov@hawaii.edu

Abstract

***Abstract**: The minimum- fuel optimal control problem for powered descent is formulated for the case of motion in a uniform gravity field. The problem is considered as part of the development of an optimal trajectory design for Mars powered descent and pin-point landing at a desired landing site. Analytical solutions for powered descent trajectory are presented. The algorithms used in the simulations have no iterative procedures nor approximations except for the assumption on the uniformity of the gravity field. These algorithms were designed to incorporate the solution of the minimum landing error problem by appropriate selection of the integration constants, maneuver time and the control parameter. The simulation results show that the analytical solutions obtained in this work can be implemented to generate feasible and extremal or optimal powered descent and landing trajectories with minimum landing error. The results were comparable to those of the studies that use convex optimization. Due to explicitness, these solutions can be used to determine manifolds of initial conditions for powered descent, to generate powered descent trajectory envelops, and to design integrated trajectory and attitude guidance.*

***Keywords**: Extremal control, real-time guidance, analytical solutions, powered descent.*

1 Introduction

This paper presents the results of the studies of the minimum- fuel optimal control and guidance problems for a planetary powered descent and landing at a specified landing site [1], [2]. Spacecraft is considered as a point mass with variable mass moving in a uniform and drag-free gravity field with gravitational

and thrust accelerations from a given initial manifold in the state space to a given landing point. Although the general theory of optimal trajectories is complete in the case of motion in the uniform gravity field, the number of studies on optimal analytical trajectory control and guidance design solutions is very limited [3]. In this work, the analytical solutions for three-dimensional, extremal and optimal powered descent and landing trajectories are presented. It is shown that the optimality conditions and the analysis of canonical equations reveal five different optimal control regimes and corresponding behavior of the switching function and the cost function for each control regime. These regimes determine the control sequence and consequently, the 14-th- order canonical system of equations are integrated completely analytically in terms of time, thereby providing 14 new arbitrary integration constants. It is shown that the integrals represent highly nonlinear relationships between the integration constants and the state and co-state variables. The studies presented in this paper describe the first attempt to demonstrate that the integration constants play an important role in the design of an envelope of the descent trajectories and in the real-time targeting and guidance design for precision landing. Qualitative analysis can be conducted without any specific numerical results to construct the envelope of descent and landing trajectories, thereby accounting for the uncertainties, such as atmospheric conditions, wind turbulences and etc. In particular, the proposed solutions can be used to determine a manifold of the initial conditions from which the lander can be guided to prescribed landing site or to its vicinity determined by a terminal manifold in the state space. One of the new utilities of the analytical solutions is that the landing site can be re-designated on-board as many times as needed by redefining the integration constants, thereby solving the real-time re-targeting problem to allow for a hazard detection and avoidance and to provide a safe pin-point landing.

A series of simulations have been conducted to demonstrate the utility of the

proposed trajectory control, targeting and guidance solutions to achieve safe and precision landing on Mars [4]. The algorithms used in the simulations do not have iterative procedure or approximations except for the numerical computation of some constants. These algorithms were designed to incorporate the solution of the minimum landing error problem by appropriate selection of the integration constants, maneuver time and the control parameters. The simulation results show that the analytical solutions obtained in this work can be implemented to generate feasible and extremal or optimal powered descent and landing trajectories with minimum landing error [5]. Feasibility of the trajectories is understood in the sense of connecting the initial and final conditions with some nonzero landing errors in the final position and velocity vectors, and satisfying the mass, control and time constraints. The results were comparable to those of the studies that use convex optimization and other numerical-analytical methods [4], [6]. Due to their explicitness, the proposed solutions can be used to determine manifolds of the initial and final conditions for atmospheric entry and powered descent, to generate the trajectory envelopes, to provide re-targeting design aimed to achieve the pin- point landing and to incorporate attitude guidance. Integration of the trajectory control, targeting and guidance solutions with attitude guidance is subject of further studies.

2 Optimal Control Problem for Powered Descent

2.1 Optimal Control Problem Statement

The minimum- fuel optimal control problem is considered as part of the optimal trajectory design problem for Mars powered descent and pin-point landing at a desired landing site [2]. Consider a spacecraft as a point with variable mass moving in a uniform gravity field with the gravity and thrust accelerations. The

equations of motion of the point are [3], [4]

$$\ddot{\mathbf{r}} = \mathbf{u} + \mathbf{g}, \qquad \dot{m} = -\alpha T \tag{1}$$

where $\mathbf{r} \in R^3$ is the state vector, $\mathbf{u} \in R^3$ is the control vector, and $\mathbf{g} = \mathbf{g}_0$ is the constant gravitational acceleration vector. Let us introduce an inertial coordinate system, $OXYZ$ with the origin, O at the Mars center of mass, m is the mass, $\alpha = 1/(I_{sp}g_e)$ is the given positive constant, I_{sp} is the specific impulse, g_e is the sea level gravitational acceleration on Earth, T is the thrust. The X-axis of this system is directed towards the point of interest, the Z-axis is directed parallel to the velocity at initial time of the powered descent maneuvers. The Y-axis completes a right-handed triad. The magnitude of the control vector, $||\mathbf{u}||$ is limited by the following constraint [4]:

$$0 < a \leq ||\mathbf{u}|| \leq b, \tag{2}$$

where a and b are the given constants. As these constants are non-zero, the descent trajectory does not include zero thrust or ballistic arcs, and consists of only thrusting arcs. The initial and final conditions are given as follows:

$$\begin{aligned} \mathbf{r}(t_i) &= \mathbf{r}_0, \\ \dot{\mathbf{r}}(t_i) &= \dot{\mathbf{r}}_0, \\ \mathbf{r}(t_f) &= \mathbf{r}_f = \mathbf{0}, \\ \dot{\mathbf{r}}(t_f) &= \dot{\mathbf{r}}_f = \mathbf{0}, \\ m(t_i) &= m_0. \end{aligned} \tag{3}$$

Here t_i and t_f are the initial and final instants of time. t_i is assumed known, but t_f is to be determined in the solution process. The components of the control vector can be given in the form: $\mathbf{u}_i = ue_i,\ i = 1, 2, 3$, where $u = ||\mathbf{u}||$, and e_i are the components of $\mathbf{e}$, the unit vector of $\mathbf{u}$. All these components are given in the system $OXYZ$. Consequently, utilizing Eq.(2), the control vector, that

is the thrust acceleration vector is to satisfy the following constraints [5]:

$$\Phi_1 = e_1^2 + e_2^2 + e_3^2 - 1 = 0, \qquad \Phi_2 = (u-a)(b-u) - \eta^2 = 0, \tag{4}$$

where η_2 is the unknown slack variable. In this case, the control vector-function is extended to have the following components: u, e_i $(i = 1, 2, 3), \eta$. The performance index of the problem is given as

$$J = \int_{t_i}^{t_f} ||\mathbf{u}|| dt. \tag{5}$$

Now the problem under consideration can be stated as follows: it is required to find the state vector, $\mathbf{x}(\mathbf{r}, \dot{\mathbf{r}}, m)$, and $\mathbf{u}$ that can satisfy Eqs.(1)- (4) and minimize the performance index, J, given in Eq.(5).

2.2 First - Order Optimality Conditions

By defining $\mathbf{r} = \mathbf{r}(x_1, x_2, x_3)$, $\mathbf{v} = \mathbf{v}(v_1, v_2, v_3)$ and $\mathbf{g} = \mathbf{g}(g_1, g_2, g_3)$, where the components of the vectors are given in the $OXYZ$ coordinate system, and accepting that $T = mu$, Eqs.(1) can be rewritten in the following first-order form $(i = 1, 2, 3)$:

$$\begin{aligned} \dot{r}_i &= v_i, \\ \dot{v}_i &= ue_i + g_i, \\ \dot{m} &= -\alpha m u. \end{aligned} \tag{6}$$

The corresponding boundary conditions, Eqs.(3) are

$$\begin{aligned} \mathbf{r}(t_i) &= \mathbf{r}_0, \\ \mathbf{v}(t_i) &= \mathbf{v}_0, \\ \mathbf{r}(t_f) &= \mathbf{r}_f = \mathbf{0}, \\ \mathbf{v}(t_f) &= \mathbf{v}_f = \mathbf{0}, \\ m(t_i) &= m_0. \end{aligned} \tag{7}$$

If

$$\mathbf{x} = \mathbf{x}(\mathbf{r}, \mathbf{v}, m), \qquad \boldsymbol{\lambda} = \boldsymbol{\lambda}(\boldsymbol{\lambda}_v, \boldsymbol{\lambda}_r, \lambda_m),$$

then the extremality conditions for the problem Eqs.(1) - (5) can be written in the form [6]:

$$\dot{\mathbf{x}} = \left[\frac{\partial H}{\partial \boldsymbol{\lambda}}\right]^T, \qquad \dot{\boldsymbol{\lambda}} = -\left[\frac{\partial H}{\partial \mathbf{x}}\right]^T \tag{8}$$

where the Pontryagin function, H is given as

$$H = \sum \lambda_i(ue_i+g_i) - \lambda_m \alpha m u + \mu_1[e_1^2+e_2^2+e_3^2-1] + \mu_2[(u-a)(b-u)-\eta^2] + \lambda_0 u. \tag{9}$$

Here μ_1 and μ_2 are additional slack variables, and λ_0 is assumed to be a non-zero Lagrange multiplier associated with the integrand function of Eq.(5). The second half of Eq.(9) can be re-written in the form:

$$\begin{aligned} \dot{\lambda}_i &= -\frac{\partial H}{\partial v_i} = -\lambda_{i+3}, \\ \dot{\lambda}_{i+3} &= -\frac{\partial H}{\partial x_i} = -\sum_j \lambda_j \frac{\partial g_j}{\partial x_i}, \\ \dot{\lambda}_m &= \lambda_m \alpha u. \end{aligned} \tag{10}$$

In addition to Eqs.(10), the extremality of H with respect to the control variables can be expressed with the following conditions:

$$\begin{aligned} \frac{\partial H}{\partial e_i} &= \lambda_i u + 2\mu_1 e_i = 0, \\ \frac{\partial H}{\partial u} &= \sum \lambda_i e_i - \lambda_m \alpha m + \mu_2(a+b-2u) + \lambda_0 = 0, \\ \frac{\partial H}{\partial \eta} &= -2\mu_2 \eta = 0. \end{aligned} \tag{11}$$

Eqs.(6) and (10) can be used to find all 14 components of $\mathbf{x}$ and $\boldsymbol{\lambda}$, and Eqs.(11) can serve to determine the control variables, e_i, u and η by employing the Weierstrass condition. Note that without loss of generality, one can choose λ_0 to be $\lambda_0 = 1$.

3 Lagrange Multipliers and Optimal Control Regimes

Note that $\mathbf{g} = \mathbf{g}(g_1, g_2, g_3)$ is a constant vector, which can be determined as $\mathbf{g} = \mathbf{g}(-g_0,\ 0,\ 0)$, where $g_0 = ||\mathbf{g}|| = const$. Consequently, taking into account that α is also a constant parameter, the equations of Eqs.(10) can be integrated as

$$\begin{aligned} \lambda_i &= a_i t + b_i, \quad i = 1, 2, 3; \\ \lambda_{i+3} &= a_i, \quad i = 1, 2, 3; \\ \lambda_m &= \lambda_{m0} \exp[\alpha \int u dt], \end{aligned} \tag{12}$$

where $a_i,\ b_i$ $(i = 1, 2, 3)$ and λ_{m0} are the integration constants. The first group of formulas of Eqs.(12) show that

$$\boldsymbol{\lambda}_v = \mathbf{a}t + \mathbf{b}, \tag{13}$$

the **p**-trajectory or the hodograph of the primer vector, $\boldsymbol{\lambda}_v(\lambda_1, \lambda_2, \lambda_3)$ is a straight line, which passes through zero if all constants b_i $(i = 1, 2, 3)$ are zeros. λ is the distance from the origin of the coordinate system with axes $\lambda_1, \lambda_2, \lambda_3$ to the hodograph. At the same time, not all a_i and b_i (i=1,2,3) can be zeros. In general, the magnitude

$$\lambda = \sqrt{\lambda_1^2 + \lambda_2^2 + \lambda_3^2} = ||\boldsymbol{\lambda}_v||$$

is a monotonic, and either increasing or decreasing function of time.

As is known, the Weierstrass condition can be given in the form:

$$\lambda_i \dot{x}_i \geq \lambda_i \dot{x}_i^*,$$

where $\dot{x}_i$ are computed on the optimal trajectory, and $\dot{x}_i^*$ are computed on the admissible trajectory. For the problem Eqs.(1)- (5) this condition has the form:

$$u(\sum \lambda_i e_i - \lambda_m \alpha m) \geq u^*(\sum \lambda_i e_i^* - \lambda_m \alpha m). \tag{14}$$

If $\eta = 0$ and $u = a$ (see Eqs.(4)), then Eq.(14) can only be satisfied if $(\sum \lambda_i e_i - \lambda_m \alpha m) \leq 0$. In the same manner, if $\eta = 0$ and $u = b$, then Eq.(14) can be

satisfied if $(\sum \lambda_i e_i - \lambda_m \alpha m) \geq 0$. If $\eta \neq 0$ and $a < u < b$, then Eq.(14) can be satisfied if $(\sum \lambda_i e_i - \lambda_m \alpha m) = 0$ over a non-zero interval of time, on which u takes intermediate values: $a < u < b$. Based on these analysis, one can determine

$$\chi = \sum \lambda_i e_i - \lambda_m \alpha m$$

as a switching function. Consequently, there may exist three options for the control regimes:

$$(1)\ u = a \quad if \quad \chi \leq 0; \quad (2)\ u = b \quad if \quad \chi \geq 0; \quad (3)\ a < u < b \quad if \quad \chi \equiv 0. \tag{15}$$

From the last equation of Eqs.(11), one can find that there may exist three cases:

1. If $\mu_2 = 0,\ \eta \neq 0$, then there may exist a variable u, such that $a < u < b$. In this case, from the second equation of Eqs.(11) and from Eqs.(15) it can be see that $\lambda_0 = 0$ which contradicts to the assumption made above that $\lambda_0 \neq 0$.

2. If $\mu_2 \neq 0,\ \eta = 0$, then from Eqs.(4) it can be seen that u takes boundary values: $u = a$ or $u = b$.

3. If $\mu_2 = 0,\ \eta = 0$, then one can obtain the same contradiction as described in the case 1.

Consequently, an optimal trajectory of the problem Eqs.(1)- (5) includes on the the thrust arcs with boundary values of the control function: $u = a$ or $u = b$. The intermediate values of the control are not optimal.

From the first group of equations of Eqs.(11), it can be seen that μ_1 can be chosen to show that $\boldsymbol{\lambda} || \mathbf{e}$, or simply,

$$e_i = \lambda_i / \lambda, \quad i = 1, 2, 3. \tag{16}$$

In this case one can find that $\chi = \lambda - \lambda_m \alpha m$ and $\dot{\chi} = \dot{\lambda}$. Consequently, from Eq.(13) it follows that, in general, there may exist the following cases (see Fig.1):

(a) λ decreases $\forall t \in [t_i, t_f]$, and it may or may not reach its minimum value. This case means that λ decreases from t_i until t_f, and $t_f \leq t^*$, where t^* is the time instant at which λ reaches its minimum value. In this case, $\dot{\lambda} \leq 0$ and $\dot{\chi} \leq 0 \ \ \forall t \in [t_i, t_f]$ and correspondingly, χ is decreasing function of time and may cross zero only at once. So, either $\chi > 0$ or $\chi < 0$ or $\chi > 0, \ \chi < 0$ $\forall t \in [t_i, t_f]$. Correspondingly, the control regime is either $u = b$ or $u = a$ or $u = b, \ u = a \ \ \forall t \in [t_i, t_f]$ respectively. If $t_f = t^*$, then $\dot{\lambda}(t_f) = \dot{\chi}(t_f) = 0$.

(b) λ increases $\forall t \in [t_i, t_f]$, and it may or may not start from its minimum value. This case means that λ increases from $t_i \geq t^*$ until t_f. In this case, $\dot{\lambda} \geq 0$ and $\dot{\chi} \geq 0 \ \ \forall t \in [t_i, t_f]$, and so χ is increasing function of time and may cross zero only at once. As in the previous case, either $\chi > 0$ or $\chi < 0$ or $\chi < 0, \ \chi > 0 \ \ \forall t \in [t_i, t_f]$. Correspondingly, the control regime is either $u = b$ or $u = a$ or $u = a, \ u = b \ \ \forall t \in [t_i, t_f]$ respectively. If $t_i = t^*$, then $\dot{\lambda}(t_i) = \dot{\chi}(t_i) = 0$.

(c) λ decreases from t_i to t^*, reaches its minimum value at t^*, then increases from t^* to t_f. So, $\dot{\lambda} = \dot{\chi} < 0 \ \ \forall t \in [t_i, t^*]$, then $\dot{\lambda}(t^*) = \dot{\chi}(t^*) = 0$, and then $\dot{\lambda} = \dot{\chi} > 0 \ \ \forall t \in [t^*, t_f]$. So, χ can cross zero once (cases c1 and c2 below) or twice (case c3) with following sequences:

(c1) $\chi(t) > 0 \ \ \forall t \in [t_i, t_1^*]; \ \ \chi(t_1^*) = 0; \ \ \chi(t) < 0 \ \ \forall t \in [t_1^*, t^*]; \ \ \dot{\chi}(t^*) = 0; \ \chi(t) < 0 \ \ \forall t \in [t^*, t_f]$. The corresponding control regime has the following sequence: $u = b, \ u = a$.

(c2) $\chi(t) < 0 \ \ \forall t \in [t_i, t^*]; \ \ \dot{\chi}(t^*) = 0; \ \ \chi(t) < 0 \ \ \forall t \in [t^*, t_1^*]; \ \ \chi(t_1^*) = 0; \ \ \chi(t) > 0 \ \ \forall t \in [t_1^*, t_f]$. The corresponding control regime has the following sequence: $u = a, \ u = b$.

(c3) $\chi(t) > 0 \ \ \forall t \in [t_i, t_1^*]; \ \ \chi(t_1^*) = 0; \ \ \chi(t) < 0 \ \ \forall t \in [t_1^*, t^*]; \ \ \dot{\chi}(t^*) = 0; \ \chi(t) < 0 \ \ \forall t \in [t^*, t_2^*]; \ \chi(t_2^*) = 0; \ \ \chi(t) > 0 \ \ \forall t \in [t_2^*, t_f]$. Corresponding control regime has the following sequence: $u = b, \ u = a, \ u = b$.

To summarize, an optimal trajectory in the problem Eqs.(1)- (5) may have one of the following regimes for control:

Case 1: $u = a \ \ \forall t \in [t_i, t_f]$.

Case 2: $u = b \ \ \forall t \in [t_i, t_f]$.

Case 3: $u = b \ \ \forall t \in [t_i, t_1^*]; \ \ u = a \ \ \forall t \in [t_1^*, t_f]$

Case 4: $u = a \ \ \forall t \in [t_i, t_1^*]; \ \ u = b \ \ \forall t \in [t_1^*, t_f]$

Case 5: $u = b \ \ \forall t \in [t_i, t_1^*], \ \ u = a \ \ \forall t \in [t_1^*, t_2^*]$, and $u = b \ \ \forall t \in [t_2^*, t_f]$.

4 Optimal Trajectory Arcs

First, let us re-write the boundary conditions, Eqs.(7) in the form:

$$\begin{aligned} \mathbf{r}_0 &= \mathbf{r}_0(x_{10}, x_{20}, x_{30}), \\ \mathbf{v}_0 &= \mathbf{v}_0(v_{10}, v_{20}, v_{30}), \\ \mathbf{r}_f &= \mathbf{r}_f(x_{11}, x_{21}, x_{31}), \\ \mathbf{v}_f &= \mathbf{v}_f(v_{11}, v_{21}, v_{31}), \\ m(t_i) &= m_0. \end{aligned} \tag{17}$$

Using Eqs.(16) and (12), one can rewrite the second group of Eqs.(6) in the form:

$$\begin{aligned} \dot{v}_1 &= \frac{(a_1 t + b_1)u}{\lambda} - g_0, \\ \dot{v}_2 &= \frac{(a_2 t + b_2)u}{\lambda}, \\ \dot{v}_3 &= \frac{(a_3 t + b_3)u}{\lambda}, \end{aligned} \tag{18}$$

where

$$\lambda = \sqrt{k_1 t^2 + k_2 t + k_3},$$

$$k_1 = a_1^2 + a_2^2 + a_3^2, \quad k_2 = 2(a_1 b_1 + a_2 b_2 + a_3 b_3), \quad k_3 = b_1^2 + b_2^2 + b_3^2.$$

Taking into account that the control variable takes the boundary values, that is either $u = a$ or $u = b$ or $u = b,\ u = a$ and $u = b$, one can integrate Eqs.(18) in the following form:

$$\begin{aligned} v_1 &= A_1 u - g_0 t + v_{10}, \\ v_2 &= A_2 u + v_{20}, \\ v_3 &= A_3 u + v_{30}, \end{aligned} \tag{19}$$

where

$$A_i = \bar{A}_i + A_{i0}, \qquad i = 1, 2, 3. \tag{20}$$

with

$$\bar{A}_i = \frac{a_i}{k_1}\lambda + \left(\frac{b_i}{\sqrt{k_1}} - \frac{a_i k_2}{2\sqrt{k_1^3}}\right)\ln(2\lambda\sqrt{k_1} + 2k_1 t + k_2),$$
$$A_{i0} = -\bar{A}_i(t_0)$$

By substituting Eqs.(19 into the first group of Eqs.(6), the latter can be integrated in the form:

$$\begin{aligned} x_1 &= B_1 u - \frac{g_0}{2}t^2 + v_{10}t + x_{10}, \\ x_2 &= B_2 u + v_{20}t + x_{20}, \\ x_3 &= B_3 u + v_{30}t + x_{30}, \end{aligned} \tag{21}$$

where

$$B_i = \bar{B}_i + B_{i0}, \qquad i = 1, 2, 3.$$

with

$$\bar{B}_i = \frac{a_i}{k_1}\left[\frac{2k_1 t + k_2}{4k_1}\lambda + \frac{4k_1 k_3 - k_2^2}{8\sqrt{k_1^3}}\ln(\tau)\right] +$$
$$\left(\frac{b_i}{\sqrt{k_1}} - \frac{a_i k_2}{2\sqrt{k_1^3}}\right)\left[\frac{\tau(\ln\tau - 1)}{4k_1} + \frac{k_2^2 - 4k_1 k_3}{4k_1}\frac{\ln\tau + 1}{\tau}\right]. \tag{22}$$
$$B_{i0} = -\bar{B}_i(t_0).$$

Here

$$\tau = 2\lambda\sqrt{k_1} + 2k_1 t + k_2.$$

As u is constant ($u = a$ or $u = b$), the last equations of Eqs.(6) and (12) can be integrated to obtain the mass and corresponding Lagrange multiplier:

$$m = m_0 \exp[-\alpha u t], \tag{23}$$

$$\lambda_m = \lambda_{m0} \exp[\alpha u t], \tag{24}$$

where λ_{m0} is the integration constant. The performance index in Eq.(5) of the problem can now be computed in a form depending on which case among the cases (1-5) is under consideration (see Fig.1):

Case 1: $u = a \ \ \forall t \in [t_i, t_f]$:

$$J = a(t_f - t_i). \tag{25}$$

Case 2: $u = b \ \ \forall t \in [t_i, t_f]$:

$$J = b(t_f - t_i). \tag{26}$$

Case 3: $u = b \ \ \forall t \in [t_i, t_1^*]$; $u = a \ \ \forall t \in [t_1^*, t_f]$

$$J = b(t_1^* - t_i) + a(t_f - t_1^*). \tag{27}$$

Case 4: $u = a \ \ \forall t \in [t_i, t_1^*]$; $u = b \ \ \forall t \in [t_1^*, t_f]$

$$J = a(t_1^* - t_i) + b(t_f - t_1^*). \tag{28}$$

Case 5: $u = b \ \ \forall t \in [t_i, t_1^*]$, $u = a \ \ \forall t \in [t_1^*, t_2^*]$, and $u = b \ \ \forall t \in [t_2^*, t_f]$:

$$J = b(t_1^* - t_i) + a(t_2^* - t_1^*) + b(t_f - t_2^*). \tag{29}$$

The constants a_i and b_i, $(i = 1, 2, 3)$ can be determined from Eq.(19) and (21) using Eqs.(17). Note that due to presence of λ_i, $i = 1, 2, 3$, Eq.(9) explicitly depends on time, and therefore Eqs.(8) do not possess an integral for Pontryagin function:

$$H = \sum \lambda_i (u e_i + g_i) - \lambda_m \alpha m u + \lambda_0 u. \tag{30}$$

It can be seen that the procedure of determining the constants and t_f described above is valid for each thrust arc with corresponding value of u. In the cases (3-5), the time instants, t_1^* and/or t_2^* can be found from the continuity conditions

for position, velocity and Lagrange multipliers at junction points. The analytical solutions obtained above allow us to make further progress in the complete design of powered descent. In particular, these solutions can be used to determine a manifold of the initial conditions from which the lander can be guided to prescribed landing site or to its vicinity in the case of landing errors. Qualitative analysis can be conducted to generate an envelope of descent and landing trajectories which can be formulated explicitly. Another important aspect of this topic is the design of attitude guidance, and as the lagrange multipliers and corresponding trajectory solutions are determined explicitly, the trajectory guidance design can easily facilitate or incorporate the attitude guidance.

5 Extremal Guidance Solutions

5.1 Guidance Problem Statement

The guidance problem can be formulated as follows: assume that at current instant, t_c the optimal state is given by $x(t_c)$, where c is an arbitrary index. Then it is required to find a new optimal control at each sample time that would guide the spacecraft from its current position at instant t_c to the desired position, $x(t_d)$ at instant t_d by satisfying all conditions of the optimal control problem. Obviously, t_d can be considered as the final time, t_f.

5.2 Guidance solutions

The extremal guidance solutions are based on the closed-form solutions presented in Eqs.(19) - (24). Using Eqs.(30) and the transversality condition

$$H(t_f) = \left[\sum a_i v_i + \sum (a_i t + b_i)(u\frac{(a_i t + b_i)}{\lambda} + g_i) - \lambda_m \alpha m u + \lambda_0 u\right]_{t=t_f} = \frac{\partial J}{\partial t_f}, \tag{31}$$

where without loss of generality it is accepted that $\lambda_0 = 1$, one can find λ_{mf}:

$$\lambda_{mf} = \frac{1}{\alpha m_f u}\left[\sum a_i v_i + \sum (a_i t_f + b_i)\left(u\frac{(a_i t_f + b_i)}{\lambda(t_f)} + g_i\right) - u\right] \tag{32}$$

Let us assume that at an arbitrarily given instant, t_c the position and velocity vector components are given by x_{ic} and $v_{ic},\ i = 1, 2, 3$. Then the desired (final) position and velocity vectors at instant t_d can be computed using Eqs.(19) and (21) in the form:

$$\begin{aligned} v_{1d} &= A_1(t_d)u - g_0 t_d + v_{1c}, \\ v_{2d} &= A_2(t_d)u + v_{2c}, \\ v_{3d} &= A_3(t_d)u + v_{3c}, \end{aligned} \tag{33}$$

$$\begin{aligned} x_{1d} &= B_1(t_d)u - \frac{g_0}{2}t^2 + v_{1c}t + x_{1c}, \\ x_{2d} &= B_2(t_d)u + v_{20}t + x_{2c}, \\ x_{3d} &= B_3(t_d)u + v_{30}t + x_{3c}, \end{aligned} \tag{34}$$

These equations allow us to find the coefficient functions A_i and $B_i,\ i = 1, 2, 3$:

$$\begin{aligned} A_1(t_d) &= \frac{1}{u}(v_{1d} - v_{1c} + g_0 t_d), \\ A_2(t_d) &= \frac{1}{u}(v_{2d} - v_{2c}), \\ A_3(t_d) &= \frac{1}{u}(v_{3d} - v_{3c}), \\ B_1(t_d) &= \frac{1}{u}(x_{1d} - x_{1c} - v_{1c}t_d + g_0 t_d^2 2), \\ B_2(t_d) &= \frac{1}{u}(x_{2d} - x_{2c} - v_{2c}t_d), \\ B_3(t_d) &= \frac{1}{u}(x_{3d} - x_{3c} - v_{3c}t_d). \end{aligned} \tag{35}$$

$$\tag{36}$$

Also, by equating Eqs.(24) evaluated at $t_d = t_f$ and (32), one can obtain

$$\frac{1}{\alpha m_f u}\left[\sum a_i v_i + \sum (a_i t_d + b_i)\left(u\frac{(a_i t_d + b_i)}{\lambda(t_d)} + g_i\right) - u\right] = \lambda_{m0}\exp[\alpha u t_d], \tag{37}$$

wher it can be assumed that $t_d = t_f$. Eqs.(35) and (39) allow as to find unknowns $a_i,\ b_i\ (i = 1, 2, 3)$ and t_d in the form, which is generally represented as

$$\begin{aligned} t_d &= t_d(x_{1c}, x_{2c}, x_{3c}, v_{1c}, v_{2c}, v_{3c}, x_{1d}, x_{2d}, x_{3d}, v_{1d}, v_{2d}, v_{3d}, u, t_c), \\ a_i &= a_i(x_{1c}, x_{2c}, x_{3c}, v_{1c}, v_{2c}, v_{3c}, x_{1d}, x_{2d}, x_{3d}, v_{1d}, v_{2d}, v_{3d}, u, t_d, t_c), \\ b_i &= b_i(x_{1c}, x_{2c}, x_{3c}, v_{1c}, v_{2c}, v_{3c}, x_{1d}, x_{2d}, x_{3d}, v_{1d}, v_{2d}, v_{3d}, u, t_d, t_c) \end{aligned} \tag{38}$$

Then the commanded thrust acceleration, $a_{ci},\ i = 1, 2, 3$ at instant t_c can be formulated as follows:

$$a_{ci} = \frac{a_i t_c + b_i}{\lambda(t_c)} u, \qquad i = 1, 2, 3. \tag{39}$$

6 Simulations

The analytical solutions trajectories presented above have been used to simulate a Mars EDL descent and landing trajectory using the initial conditions used in Ref.[4]. The results for position, velocity and mass obtained here are comparable to those of Ref.[4], especially the results of case 1 considered in this reference. All simulations have been conducted in Matlab. As the solutions show, the main procedure is the search for the constants $a_1,\ b_1,\ a_2,\ b_2,\ a_3$ and b_3 for given simulation time, t_1 and control parameter, u. Assuming that the control parameter is the thrust acceleration, the following inequality is used [4]:

$$\frac{\rho_1}{m} \leq \sigma \leq \frac{\rho_2}{m}$$

with

$$m_{dry} \leq m_1 \leq m < m_0 = m_{wet}, \qquad m_1 = m(t_1).$$

where ρ_1 and ρ_2 are the boundary values of thrust. So practically,

$$u \leq u_{max} = \sigma_{max} = \frac{\rho_2}{m_{wet}}.$$

As the mass changes exponentially, the simulation time was computed according to the condition:

$$[t_1]_{min} = \frac{1}{\alpha u_{max}} \ln \frac{m_0}{m_1}.$$

The following values of the parameters and terminal conditions are used:

$$g0 = 3.7114, \quad m_{dry} = 1505, \quad m_{wet} = 1905, \quad \alpha = 4.5 \times 10^{-4},$$

$$\rho_1 = 4972, \quad \rho_2 = 13260, \quad \sigma_{max} = \frac{\rho_2}{m_{dry}}, \quad \sigma_{min} = \frac{\rho_1}{m_{wet}},$$

$$u_{max} = \sigma_{max}, \quad u_{min} = \sigma_{min}.$$

$$x_{10} = 1500.0, \quad x_{20} = 500.0, \quad x_{30} = -2000.0,$$

$$v_{10} = -75.0, \quad v_{20} = 0, \quad v_{30} = 100.0$$

$$x_{11} = 0, \quad x_{21} = 0, \quad x_{31} = 0, \quad v_{11} = 0, \quad v_{21} = 0, \quad v_{31} = 0,$$

$$15 \leq a_1 \leq 35, \quad 1 \leq b_1 \leq 10,$$

$$a_2 = 0, \quad b_2 = 0,$$

$$-13 \leq a_3 \leq -11, \quad -10 \leq b_3 \leq -1,$$

$$u_{min} \leq u \leq u_{max},$$

$$0 \leq t \leq 55.$$

In particular, the following values have been used:

$$a_1 = 35, \quad b_1 = 4, \quad a_2 = 0, \quad b_2 = 0,$$

$$a_3 = -13, \quad b_3 = -5, \quad u = 5.69, \quad 0 \leq t \leq 50$$

Here, the position, velocity, accelerations and mass are measured in *meters, meters/sec, meters/sec*^{2} and *kg* respectively, and these units will be omitted for simplicity. Only elementary algebraic functions and a very simple search algorithm were used to simulate the descent trajectories. The algorithms used in the simulations do not use any iterations, function calls or approximations except for the uniform gravity field, which is a reasonable approximation for

maneuvers in the vicinity of the Mars surface. The preliminary results of the simulations are presented in figures 2-5. Figures 2 and 3 demonstrate that the analytical solutions can generate feasible and extremal descent and landing trajectory envelops and the parameter domains. This means that any of the values of the coefficients from the given domains can provide an extremal or optimal trajectory. The extremality is understood in the sense of satisfying the necessary conditions of optimality with performance index given as $J = u(t_f - t_i)$, where $u = const$. In this sense, these descent trajectories considered can be optimal if the final conditions are met exactly with appropriate selection of the control, u. Feasibility of the trajectories is understood in the sense of connecting the initial and final conditions with some nonzero landing errors in the final position and velocity vectors, and satisfying the mass, control and time constraints as well as an engineering intuition. Although the purpose of the optimal control problem was to minimize J, the algorithms were also designed *to minimize the landing errors in position and velocity.* This is done by searching for not only the constants $a_1,\ b_1,\ a_2,\ b_2,\ a_3$ and b_3, but also for the appropriate simulation time, t_1 and the control parameter, u to achieve the minimum landing errors. The visual analysis of the boundaries of the trajectory envelops expose the largest landing errors of 1200 m in position and as high as 20 m/s in velocity. But it can be easily seen that by appropriate selection of the coefficients and the control parameter and the final time, these errors can be minimized to a some degree of satisfaction of the final conditions. Indeed, figures 4 and 5 show that both position and velocity errors at landing can be decreased or in some cases, eliminated using a local search of some parameters. For Fig.4, the final values of the parameters are:

$$\mathbf{r}_1(-384.3,\ 500.0,\ -34.5), \quad \mathbf{v}_1(5.0,\ 0,\ -1.7), \quad m_1 = 1676.1, \quad t_1 = 50.0$$

For Fig.5, the final values of the parameters are:

$$\mathbf{r}_1(0.0,\ 500.0,\ 661.2), \quad \mathbf{v}_1(-7.6,\ 0,\ 0.9), \quad m_1 = 1699.8, \quad t_1 = 44.4$$

More detailed search resulted in more accurate landing parameters which are given in the Table 1 below. The last lane of the table shows that the safe landing with almost zero velocity, $|\mathbf{v}_1| = 0.0024$ m/s can be provided with the positional error of $|\mathbf{r}_1| = 465.34$ m at landing. The final mass is computed to be less than 1676 kg, which means that less than 229 kg of fuel is used to perform the descent and landing maneuver. The total maneuver time was found to be 49.60 s. The studies show that more narrow and a wider local (or even global) search for the coefficients, the maneuver time and the control parameter will yield more accurate and safe landings.

Table 1: One set of selected coefficients and landing parameters

a_1	a_3	b_1	b_3	u	t_1	$\|\mathbf{r}_1\|$	$\|\mathbf{v}_1\|$
37.70	4.90	-14.40	-4.10	5.600	49.60	464.8702	0.6984
37.79	4.90	-14.40	-4.10	5.600	49.60	464.8361	0.4789
37.00	4.70	-14.00	-4.20	5.600	49.59	463.9562	0.0290
38.00	4.80	-14.40	-4.10	5.600	49.60	465.3398	0.0024

References

[1] Yang, T. L. "Optimal Control for a Rocket in a Three-Dimensional Central Force Field," Technical Memorandum. TM-69-2011-2. May 29, 1969. Belcomm, Inc. 51 p.

[2] Wolf, A., Tooley, J.,Ploen, S., Ivanov, M., Açikmeşe, B. and Gromov, K. "Performance Trades for Mar Pin-point Landing," IEEE Aerospace Conference, Inst. of Electrical and Electronics Engineers Paper 1661, 2006.

[3] Lawden, D.F. Optimal Trajectories for Space Navigation. London. Butterworths. 1963. 126 p.

[4] Blackmore, L., Açikmeşe, B., Scharf, D.P. "Minimum-Landing-Error Powered -Descent Guidance for Mars Landing Using Convex Optimization," *AIAA Journal of Guidance, Control and Dynamics*. July-August 2010, V.33, N.4, pp.1161-1171.

[5] Azimov, D.M. and Bishop, R.H. Optimal Trajectories for Space Guidance // Annals of New York Academy of Sciences. N.1065. 2005. New York, NY. pp.189-209.

[6] Leitmann, G.*An Introduction to Optimal Control*. McGraw -Hill Book Company. New-York. 1968, 192 p.

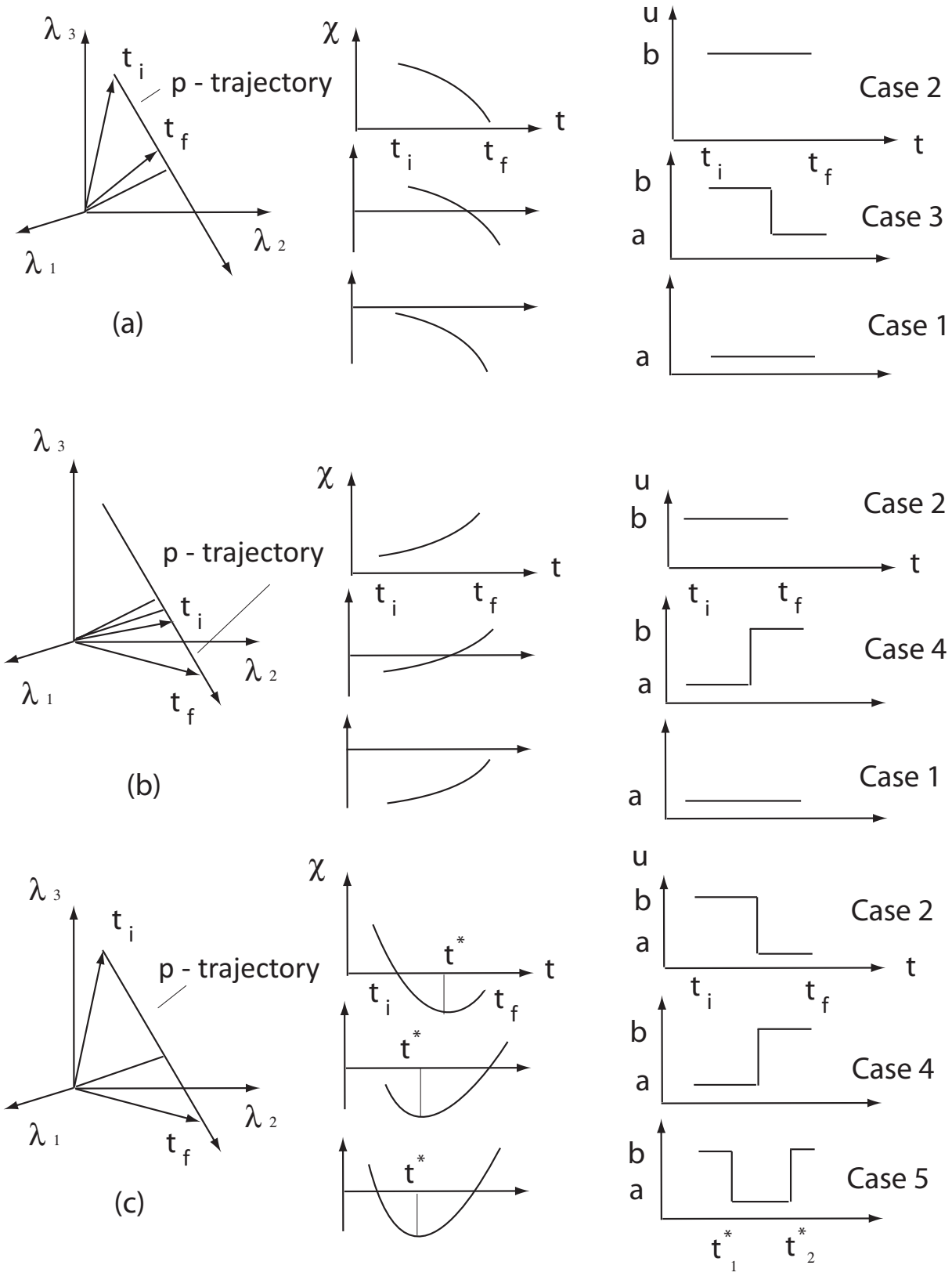

Figure 1: p-trajectory, switching function and optimal control regimes.

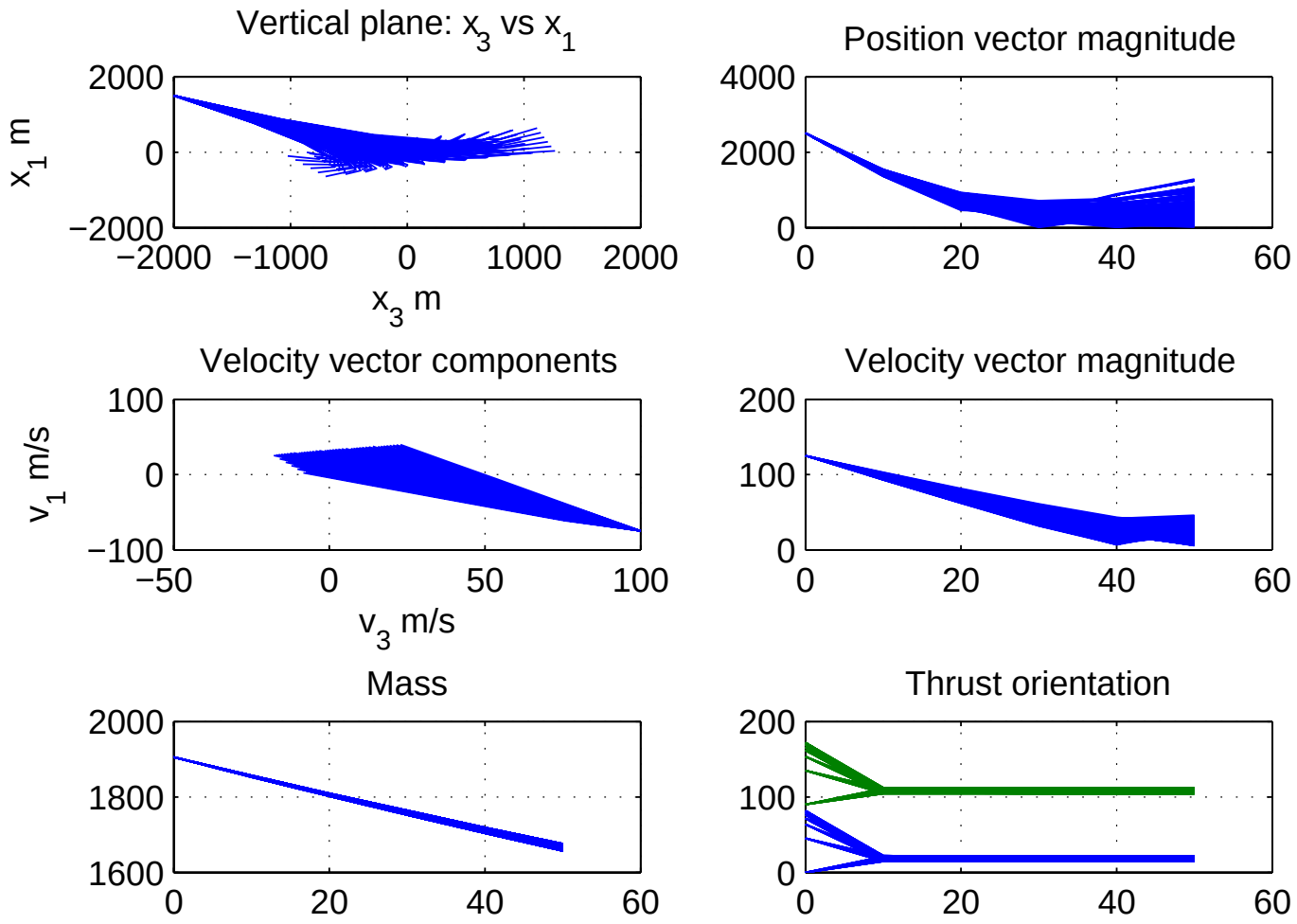

Figure 2: Descent trajectory envelops and the parameter domains: $15 \leq a_1 \leq 35, \quad 5 \leq b_1 \leq 10, \quad a_2 = 0, \quad b_2 = 0, \quad -12 \leq a_3 \leq -8, \quad -7 \leq b_3 \leq 0, \quad 5.7 \leq u \leq 6.2$

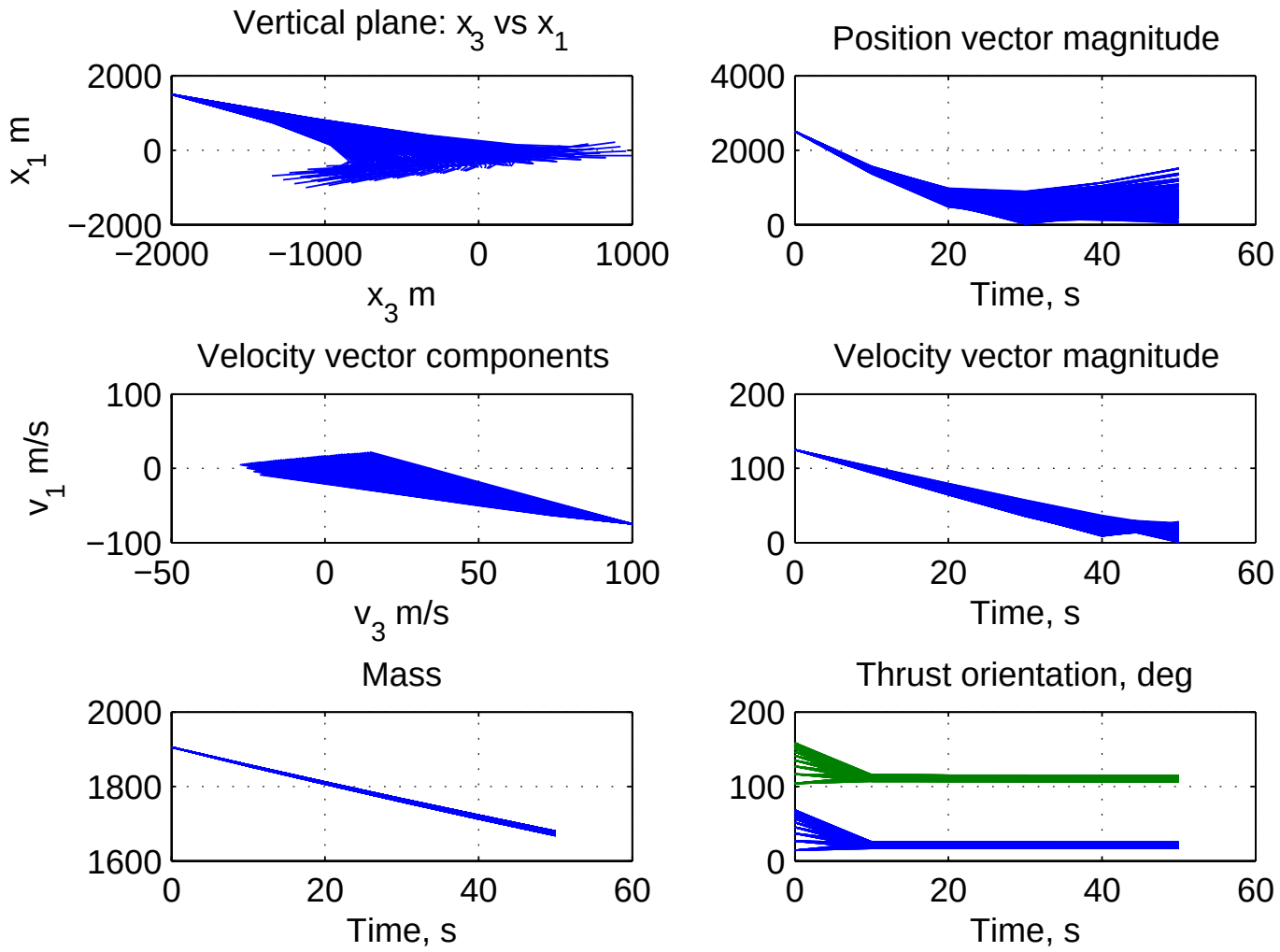

Figure 3: Descent trajectory envelops and the parameter domains: $15 \leq a_1 \leq 35, \quad 5 \leq b_1 \leq 10, \quad a_2 = 0, \quad b_2 = 0, \quad -13 \leq a_3 \leq -11, \quad -10 \leq b_3 \leq -1, \quad 5.6 \leq u \leq 5.9$

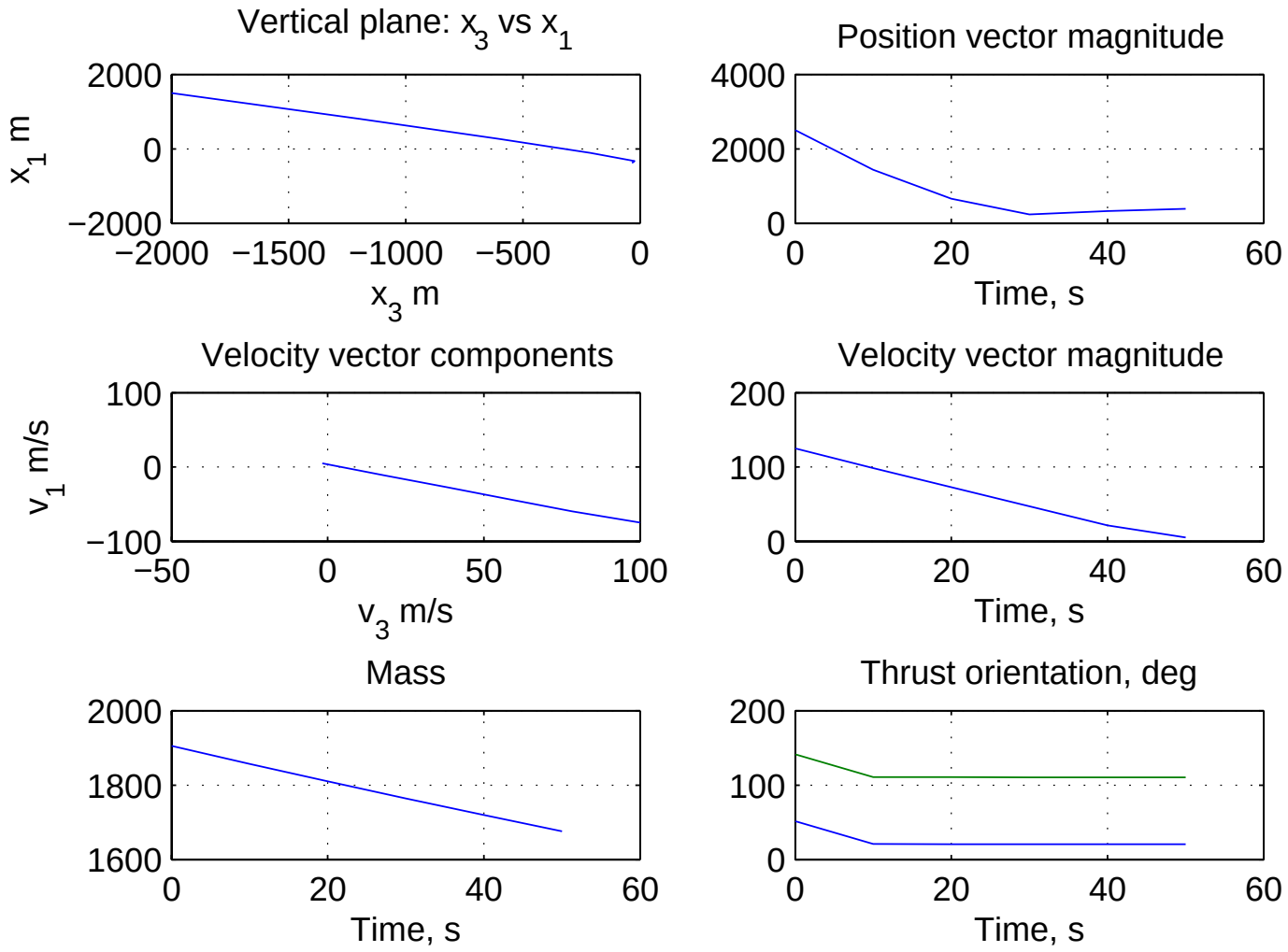

Figure 4: Descent trajectory parameters: $a_1 = 35, \quad b_1 = 4, \quad a_2 = 0, \quad b_2 = 0, \quad a_3 = -13, \quad b_3 = -5, \quad u = 5.69$.

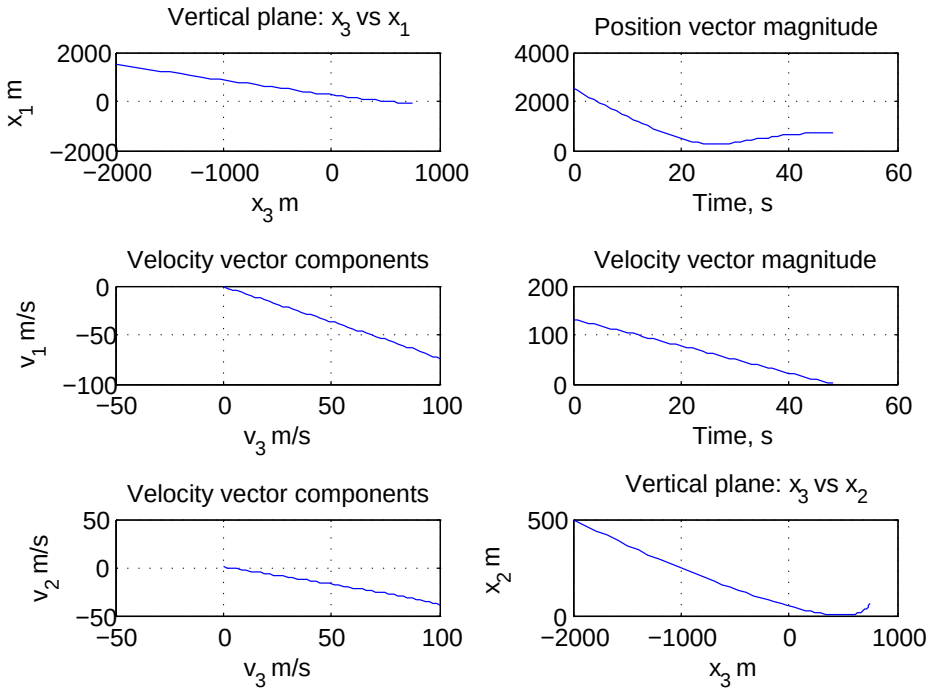
Vertical plane: x3 vs x1
x1 m
2000
0
−2000
−2000
−1000
0
1000
x3 m
Position vector magnitude
4000
2000
0
0
20
40
60
Time, s
Velocity vector components
v1 m/s
0
−50
−100
−50
0
50
100
v3 m/s
Velocity vector magnitude
200
100
0
0
20
40
60
Time, s
Velocity vector components
v2 m/s
50
0
−50
−50
0
50
100
v3 m/s
Vertical plane: x3 vs x2
x2 m
500
0
−2000
−1000
0
1000
x3 m